Solvatochromism

DOI: 10.1002/anie.201408576

Visualizing the Chain-Flipping Mechanism in Fatty-Acid Biosynthesis**

*Joris Beld, Hu Cang, and Michael D. Burkart**

Abstract: *The acyl carrier protein (ACP) from fatty acid synthases sequesters elongating products within its hydrophobic core, but this dynamic mechanism remains poorly understood. We exploited solvatochromic pantetheine probes attached to ACP that fluoresce when sequestered. The addition of a catalytic partner lures the cargo out of the ACP and into the active site of the enzyme, thus enhancing fluorescence to reveal the elusive chain-flipping mechanism. This activity was confirmed by the use of a dual solvatochromic cross-linking probe and solution-phase NMR spectroscopy. The chain-flipping mechanism was visualized by single-molecule fluorescence techniques, thus demonstrating specificity between the Escherichia coli ACP and its ketoacyl synthase catalytic partner KASII.*

Primary and secondary acetate metabolites are synthesized by dedicated fatty acid and polyketide synthases. Both families are subdivided into Type I and Type II architectures on the basis of whether they are encoded on one multidomain polypeptide chain (Type I) or as separate proteins (Type II). These synthases are often represented as molecular assembly lines with domains that catalyze reactions on the growing metabolite while tethered to an acyl carrier protein (ACP),[1] which shuttles its cargo from one enzyme to the next. Although synthetic biologists have the ambition to swap domains and modules between these synthases to create new molecular architectures, these efforts have been tempered by the discovery that both protein–substrate and protein–protein interactions play an important role in both iterative and modular assemblies.[2] Owing to the highly dynamic nature of these protein complexes, structural information on their interactions remains scarce.

Productive interactions between the ACP and its partners are required for catalysis, and the de novo design of synthases will rely on this underlying behavior. The large ACP family ($>10^6$ homologues) is structurally conserved in all kingdoms of life and spans a large sequence space.[3] All ACPs are acidic proteins of 60–100 amino acids and contain three major and one small α-helix. A highly conserved serine motif (D/W/N–S–L/M) is post-translationally modified by phosphopantetheinyl transferases (PPTases), which transform apo-ACP into its holo form by addition of the 4′-phosphopantetheine moiety from coenzyme A (CoA), the terminal thiol group of which ferries cargo during catalysis through a thioester linkage.

In type II synthases, in which enzymes are found as separate proteins, NMR spectroscopy[4] and molecular-dynamics studies[5] have demonstrated that cargo becomes sequestered in the ACP hydrophobic core between helix II and III. In contrast, type I synthases do not appear to sequester their cargo.[6] At least four different explanations have been proposed for cargo sequestration, including protection of the thioester linkage from hydrolysis and premature product release, the protection of unstable polyketides from side reactions, providing a limiting "ruler" for the control of metabolite size, and the induction of conformational changes to trigger proper catalysis.

Herein, we present a new technique based on the use of solvatochromic fluorophores for the visualization of cargo sequestration and release by ACPs and their catalytic partners (Figure 1). These dyes are highly sensitive to the environment. Their fluorescence lifetime, emission wavelength, and quantum yield vary with solvent hydrophobicity.[7] Solvatochromic dyes[8] have found important application in studies of protein structure and dynamics,[7b] and we recognized the potential utility of such environmental reporters as tags to probe ACP activity.[9] 4-*N*,*N*-Dimethylamino-1,8-napthalimide (4-DMN), which has been applied to the sensing of protein–peptide interactions,[10] displays only weak fluorescence in aqueous solution, thus making it ideal for the detection of small environmental changes.[7a] 7-Nitrobenz-2-oxa-1,3-diazol-4-yl (Nbd)[11] derivatives also show solvatochromic behavior but differ in their electronic and steric properties. These dyes, along with the control rhodamine B, which is much larger and shows limited solvatochromic behavior,[12] were fused with pantetheine analogues for attachment to ACP (Scheme 1). Computational docking predicted that the Nbd and 4-DMN pantetheine probes could be sequestered into the core of type II fatty acid synthase (FAS) ACPs (see the discussion and Table S1,

[*] Dr. J. Beld, Prof. Dr. M. D. Burkart
Department of Chemistry and Biochemistry
University of California San Diego
9500 Gilman Drive, La Jolla, CA 92093-0358 (USA)
E-mail: mburkart@ucsd.edu

Dr. H. Cang
Waitt Advanced Biophotonics Center
The Salk Institute for Biological Studies
La Jolla, California (USA)

[**] J.B. was supported by a Rubicon postdoctoral fellowship. M.D.B. and J.B. were funded by California Energy Commission CILMSF 500-10-039; DOE DE-EE0003373; NIH R01GM094924; and R01GM095970. We thank J. J. La Clair for fruitful discussions and support, X. Huang and D. J. Lee for training and support with solution protein NMR spectroscopy, and T. L. Foley (NIH) for the plasmid encoding *H. sapiens* ACP.

Supporting information for this article, including experimental details, is available on the WWW under http://dx.doi.org/10.1002/anie.201408576.

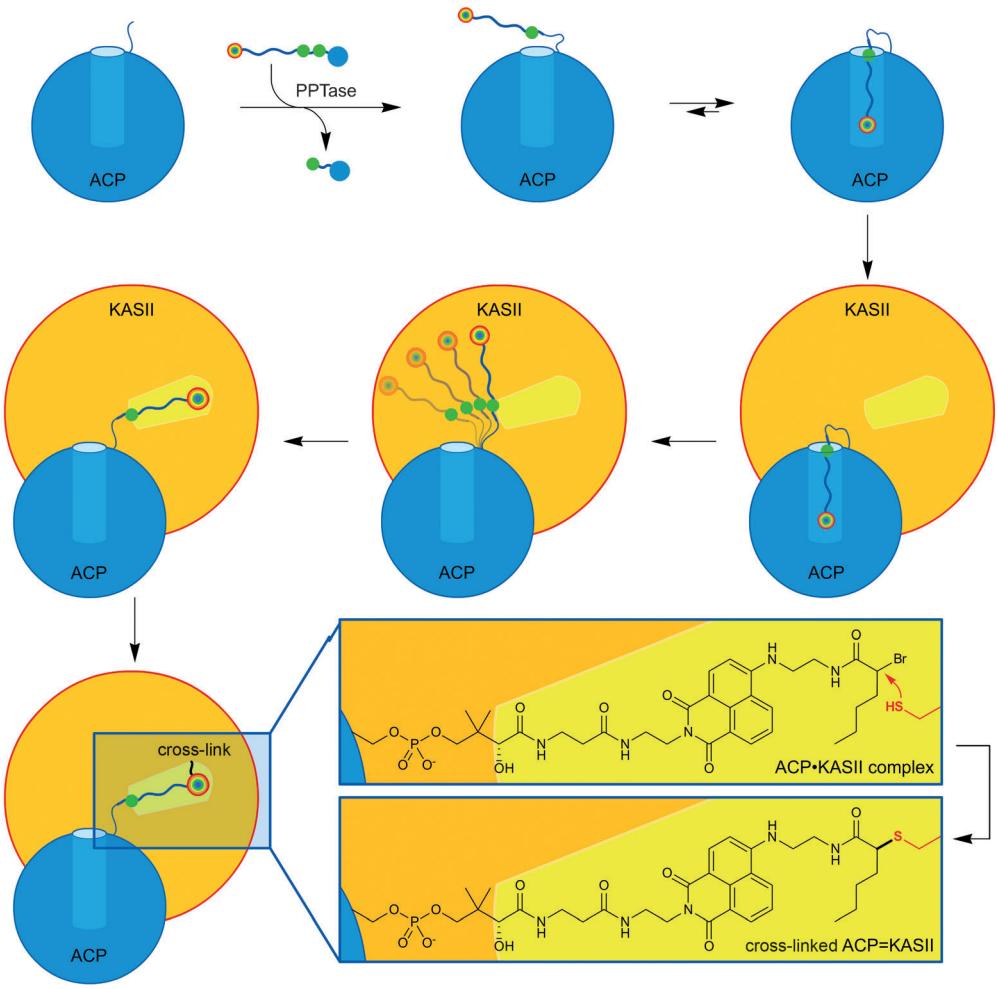

Figure 1. Chain-flipping mechanism visualized by solvatochromism. The apo-acyl carrier protein (ACP) is loaded with a solvatochromic CoA analogue by use of the promiscuous PPTase Sfp. Sequestration of the cargo in the inner core of ACP leads to a visible color and fluorescence signal. The addition of ketoacyl synthase II (KASII) reveals the chain-flipping mechanism in which the probe is extended into the active site of KASII. The cross-linking moiety on probe **4** forms a covalent bond with the active-site cysteine residue of KASII.

Table S2, Figure S1, and Figure S2 in the Supporting Information), but the larger rhodamine pantetheine probe would not. It was predicted that none of these probes could be sequestered by type I FAS ACPs. Although these solvatochromic probes do not resemble the natural fatty-acid cargo of ACPs, computational docking showed that especially small dyes, such as 4-DMN, do fit inside the inner core of ACPs of type II FASs.

Next, the synthesized pantetheine probes were loaded onto a type II FAS ACP from *Escherichia coli* (EcACP). The probes were transformed in situ into CoA analogues and subsequently installed on ACP by the 4′-phosphopantetheinyl transferase (PPTase) Sfp.[13] The loading of ACP was monitored by conformationally sensitive urea-PAGE[14] (see Figure S3), bands corresponding to labeled ACP were excised, and the proteins were electroeluted for analysis by fluorescence spectroscopy and LC–MS (see Figures S4 and S5).

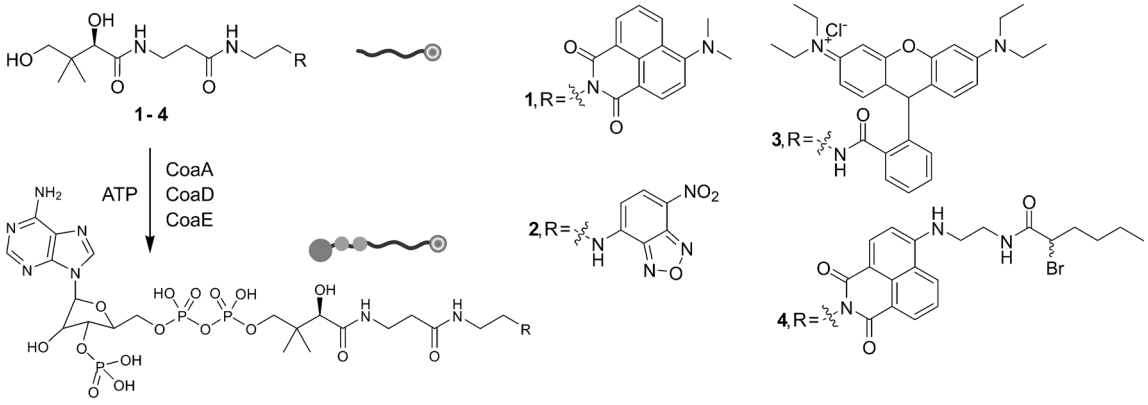

Scheme 1. Compounds used in this study. Pantetheinamide derivatives of 4-DMN (4-*N*,*N*-dimethylamino-1,8-naphthalimide; probe **1**), Nbd (7-nitrobenzo-2-oxa-1,3-diazole; probe **2**), and rhodamine B (probe **3**) were synthesized from pantothenic acid by *p*-methoxybenzyl (PMB) protection, coupling with 2-azidoethanamine, reduction, coupling with the fluorophore, and deprotection. An extended solvatochromic 4-DMN-inspired mechanistic cross-linker **4** was synthesized from a protected pantetheinamide substituted with 4-bromo-1,8-naphthalimide by treatment with ethylenediamine, coupling of 2-bromohexanoic acid, and deprotection. CoaA, CoaD, and CoaE transformed the pantetheinamides into CoA analogues, as substrates for the promiscuous PPTase Sfp, which installed these probes onto ACPs.

To evaluate our hypothesis of probe sequestration, we studied the behavior of ACPs modified with probes **1**–**3** in solution. The results could be rapidly discerned by eye, whereby an aqueous solution containing EcACP bearing 4-DMN-containing pantetheine probe **1** appeared bright yellow (see Figures S3 and S6). The addition of a denaturant (urea or sodium dodecyl sulfate, SDS) turned the solution colorless (see Figures S3 and S7) and also eliminated the fluorescence signal for **1** at 515 nm (Figure 2a), thus indicating the unfolding of the protein and exposure of the solvatochromic dye to the aqueous environment. No visible color or fluorescence was observed for apo-EcACP in its native or denatured state (see Figure S6). A high concentration of probe **1** dissolved in a buffer showed no change in fluorescence upon the addition of a denaturant but a significant increase and shift in fluorescence upon the addition of an organic solvent (CH_3CN; see Figure S7). EcACP loaded with the Nbd-containing pantetheine probe **2** showed a marked decrease and shift in fluorescence upon denaturation. In agreement with the computational docking results, EcACP loaded with the rhodamine pantetheine probe **3** showed no change in fluorescence upon denaturation, thus suggesting that the bulky probe is not sequestered (see Figure S8).

Taken together, the results with these solvatochromic-dye-loaded ACPs further demonstrate the phenomenon that EcACP sequesters cargo of moderate size inside the helix bundle. To validate these results, we turned to solution-state NMR spectroscopy. Uniformly ^{15}N-labeled apo-EcACP was loaded with probe **1** to form crypto-EcACP. Cargo sequestration by acyl-EcACP elicits significant chemical-shift perturbations in ^{15}N,^{1}H HSQC spectra as compared to the spectra of apo- and holo-EcACP.[15] Chemical-shift perturbations observed in crypto-4-DMN-EcACP (Figure 2e–g; see also Figure S9 and Table S3) are comparable to those previously observed for other sequestering crypto-EcACPs,[15] thus validating the location of the 4-DMN probe.

To extend this technique to type I ACPs, we loaded hACP excised from *Homo sapiens* FAS with the solvatochromic pantetheine probes. The excised hACP readily forms a disulfide homodimer,[16] which is not a substrate for Sfp, but the addition of dithiotreitol prevents this dimerization. Although computational modeling predicted no probe sequestration (see Tables S1 and S2), the crypto proteins showed modest fluorescence in an aqueous environment (but no visible yellow color). However, in contrast with EcACP, the addition of a denaturant did not significantly change the fluorescence (Figure 2b), thus suggesting that the probes are not sequestered but are associated with the surface of hACP. To explain this differential behavior, computational analysis of the electrostatic surface potential and hydrophobicity of hACP

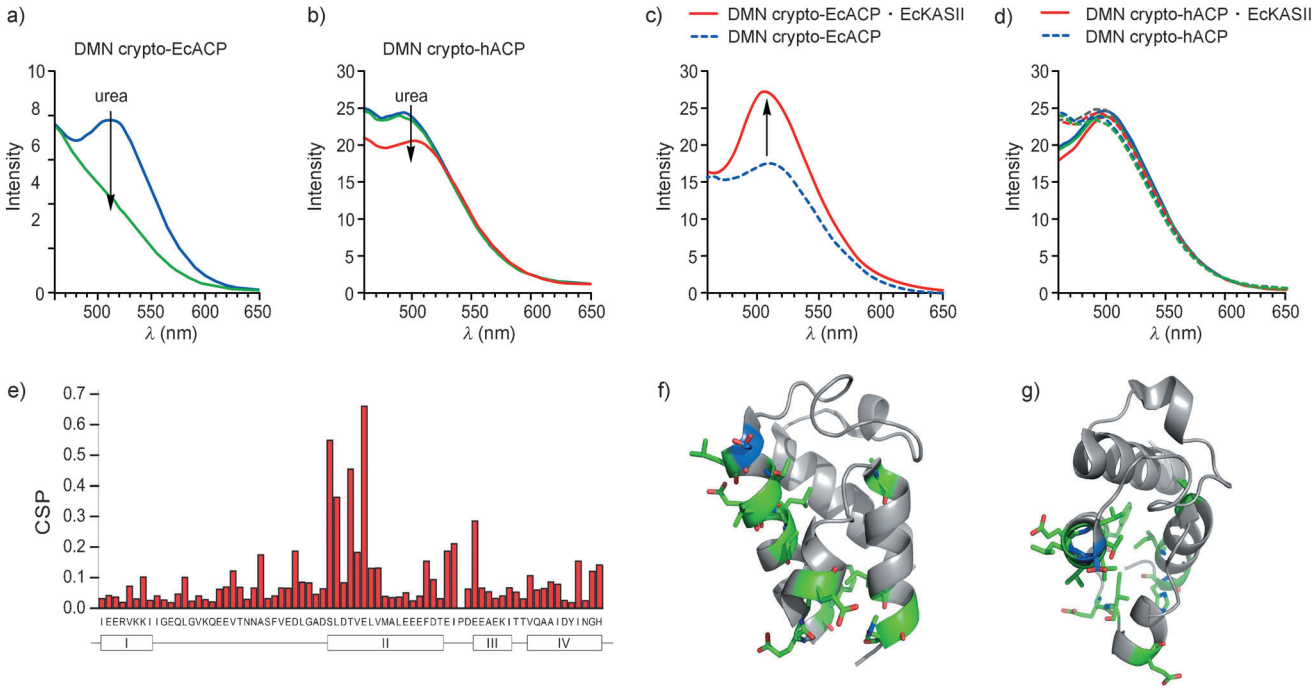

Figure 2. Solvatochromism for the elucidation of ACP dynamics. a) Denaturation of crypto-EcACP, modified with probe **1**, as measured by fluorescence spectroscopy. Upon denaturation of labeled EcACP, the sequestered probe is exposed to an aqueous buffer, thus resulting in the disappearance of the fluorescence signal and the visible yellow color of the labeled protein (see Figure S3). b) The loss of the fluorescence maximum as seen in (a) was not observed for crypto-hACP. c,d) EcKASII was titrated into EcACP (c) and hACP (d) loaded with probe **1**, as monitored by fluorescence spectroscopy. Whereas the fluorescence maximum increased in the case of labeled EcACP, labeled hACP did not respond to the addition of EcKASII. e) Comparison of holo-EcACP with crypto-EcACP (modified with probe **1**) in terms of chemical-shift perturbation (CSP) in the solution protein NMR spectra. Typical perturbations observed for helix II upon cargo sequestration provide direct evidence for the presence of probe **1** in the inner hydrophobic core of EcACP and thus its solvatochromic behavior. f, g) Side and top views of the protein structure showing perturbed residues (as green sticks). Serine 36, the residue which is 4′-phosphopantetheinylated, is shown in blue. Apo-ACP is ACP directly from the ribosome, holo-ACP is 4′-phosphopantetheinylated apo-ACP and crypto-ACP is apo-ACP modified with an unnatural 4′-phoshopantetheine analogue.

versus EcACP (see Figure S10) revealed major differences between these carrier proteins and is consistent with the localization of the dye on the protein surface.

We next examined the dynamic movement of a sequestered acyl substrate from within a type II ACP into the active site of a partner enzyme, also referred to as chain flipping.[17] This phenomenon has never been directly detected, but the protein–protein interactions governing this activity remain at the forefront of pathway engineering. Recently, two elegant studies revealed snapshots of these protein–protein interactions[17] in the form of cocrystal structures of *E. coli* ACP with partner enzymes (LpxD[18] and FabA[1]). The dynamic interaction between FabA and ACP was also investigated by NMR titration experiments; however, since the population of protein species involved in chain flipping is most likely small, this event has to date not been measured. The size of ACP–partner-protein complexes pushes standard solution protein NMR spectroscopy to its limits and requires novel NMR spectroscopic techniques, such as solution-state TROSY or solid-state magic-angle-spinning sedimentation.[19] Indeed, when we added unlabeled *E. coli* ketoacyl synthase II (EcKASII, FabF) to a solution of our labeled EcACP, severe signal broadening was observed (see Figure S9). Furthermore, protein NMR spectroscopy still often requires relatively large amounts of protein and can be time-consuming and costly. Thus, our solvatochromic approach to visualization of the chain-flipping mechanism offers a facile and orthogonal way to study ACP–partner-protein interactions.

We chose to examine ketoacyl synthase II, which extends fatty acids up to eighteen carbons.[20] Previously, we showed that EcACP loaded with chloroacrylic or α-bromo moieties can successfully interact and cross-link with EcKASII.[21] Both EcACP and hACP loaded with **1** were titrated with increasing concentrations of EcKASII, and we only observed a significant increase in fluorescence for EcACP (Figure 2c). As a negative control, EcACP was titrated with a protein that is not its partner, bovine serum albumin (BSA), which showed no effect (see Figure S11). Human ACP does not functionally interact with EcKASII (Figure 2d), as determined by a mechanistic cross-linking experiment (not shown).[21a] These findings indicate that either EcKASII induces hydrophobicity around the pantetheine probe by compaction or EcKASII is able to extrude the cargo from the ACP for binding within its hydrophobic active site. Computational docking studies indicate that the active site of EcKASII can accommodate probe **1** (see Figure S12), thus suggesting that chain-flipping activity is responsible for the increase in fluorescence.[22]

As mentioned, we recently introduced mechanistic cross-linking as a tool to capture protein–protein interactions between carrier proteins and their partners.[21a] We hypothesized that cross-linking could be used to conclusively deduce the source of the increase in the fluorescence signal upon the addition of EcKASII to EcACP loaded with probe **1**. Therefore, the solvatachromic cross-linking probe **4** was prepared, and its loading onto EcACP resulted in a yellow colored protein with a fluorescence response. The addition of EcKASII resulted in a cross-linked complex with increased fluorescence, as visualized by SDS-PAGE (see Figure S13), with a molecular weight of 54 kDa. Isolated solvatochromic cross-linked EcACP–EcKASII showed a strong fluorescence signal ($\lambda_{ex} = 408$ nm and $\lambda_{em} = 515$ nm) (see Figure S14A), although EcACP labeled with **4** itself gave a low fluorescence signal (see Figure S14B). The titration with EcKASII of EcACP labeled with **4** led to the appearance of a strong fluorescence signal, albeit only after incubation overnight (see Figure S14B). The incubation of EcKASII with **4** alone did not result in fluorescence (see Figure S14C), thus suggesting that protein–protein interactions between ACP and ketoacyl synthase are required for the binding of **4** within EcKASII. As expected, hACP loaded with **4** did not cross-link with EcKASII (data not shown). These results indicate that the solvatochromic fluorescence response with **4** is indeed a result of its transition from sequestration within EcACP to the active pocket of EcKASII. The increased fluorescence response therefore provides a direct response for chain-flipping activity.

Single-molecule fluorescence microscopy[23] is emerging as a valuable technique for studying biological processes, such as protein trafficking in living organisms and protein–protein interactions.[24] We reasoned that solvatochromic response from chain-flipping activity could be applied to single-molecule fluorescence microscopy, whereby single binding events between EcACP and EcKASII could be quantified. In this study, we attached EcKASII to a quartz surface and flowed DMN-labeled EcACP over the surface (Figure 3a) while recording a video of fluorescence events (Figure 3b). Many bright events were observed, unlike when the pantetheine probe **1** was flowed over the same surface. More than 85% of the brightest spots acquired by the camera ($\lambda_{ex} =$ 488 nm and $\lambda_{em} = 525/50$ nm) and selected by the software were distinct peaks with a clear signal intensity over background and a defined lifespan (Figure 3b), whereas the corresponding experiment with probe **1** alone resulted in some bright spots, of which less than 20% were peaks (possibly originating from aggregation). When labeled EcACP was flowed over an unmodified poly(ethylene glycol) (PEG, $M_w \approx 5$ kDa) surface, approximately 60% of the observed bright spots were peaks, but with very different intensities and "ON" time (lifespan) distribution (Figure 3b). In the case of labeled EcACP–EcKASII, the lifespan times were short and peak-intensity distributions were narrow, thus indicating that the interactions with the partner protein (KASII) changed the environment of the probe attached to EcACP significantly. Conversely, in the case of labeled EcACP flowing over an unmodified PEG surface, peak intensities were substantially increased, and the lifespan times showed more variation (Figure 3b). We also modified EcKASII with the cyanine dye Cy5 and performed a colocalization experiment with two different lasers ($\lambda_{ex} = 488$ nm and $\lambda_{ex} =$ 640 nm) in which either the Cy5-labeled EcKASII or the DMN-labeled EcACP was excited. This experiment is normally used for tight binding events; we were investigating transient interactions between ACP and KS, thus complicating the analysis. However, a nontrivial population (ca. 8%) as compared to the statistical probability (ca. 3%) showed bright fluorescence events in exactly the same location, in both channels, thus suggesting that we were indeed observing ACP–partner-protein interactions (see Figure S15). The sig-

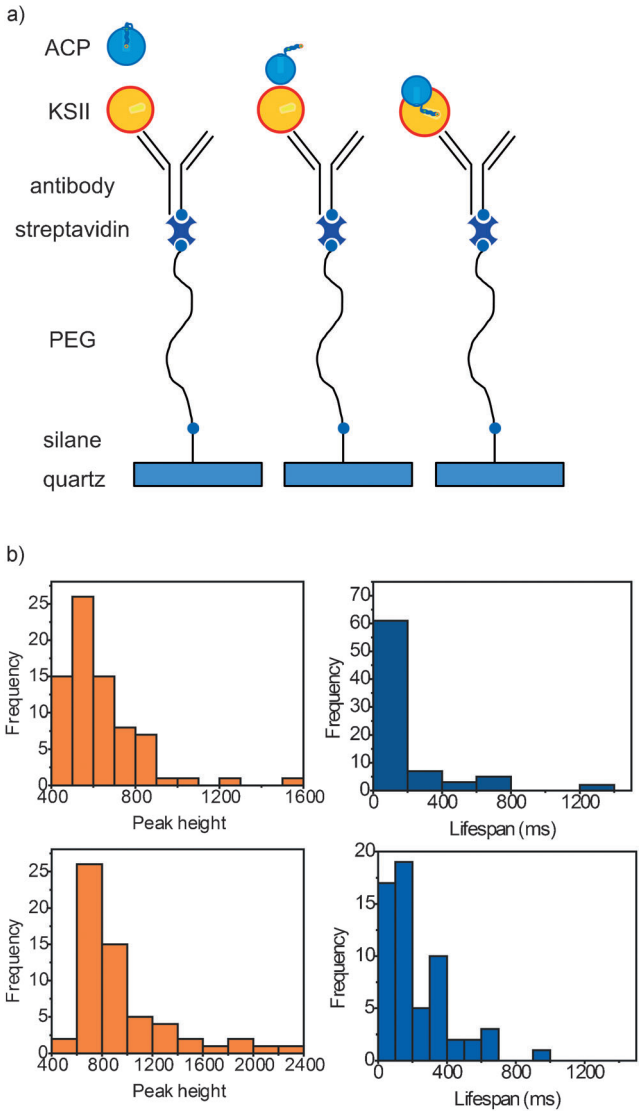

Figure 3. Single-molecule-fluorescence behavior of DMN-labeled EcACP. a) A layered design was patterned on a quartz surface to provide sufficient spacing between proteins and to prevent surface effects. A sandwich approach was used for the attachment of EcKASII on the basis of the sequential layering of aminosilane, biotinylated PEG ($M_w \approx 5$ kDa), streptavidin, biotinylated anti-$(His)_6$ antibody, and $(His)_6$-tagged EcKASII (KSII). DMN-labeled EcACP was flowed over the decorated surface, and a video recording of fluorescence events was made. b) Time-lapsed images were collected to visualize the bleaching of single molecules. Bright pixels were detected, and human analyses were performed to unselect aberrant data points. After selection, fluorescence intensity at 525/50 nm was plotted over time, and the observed peaks were analyzed. Peak height is an arbitrary value of signal intensity, and lifespan was determined from the width of the observed fluorescent peaks. Top: DMN-labeled EcACP flowed over EcKASII; bottom: DMN-labeled EcACP flowed over unmodified PEG. When the pantetheine probe **1** was flowed over EcKASII, no significant fluorescence events were observed.

nificant difference in fluorescence response at the single-molecule level functionally demonstrates chain-flipping activity triggered by protein–protein interactions between EcACP and EcKASII. We envision that it will be possible to use this single-molecule approach to rapidly screen ACP–partner-protein interactions at very low concentrations in the future.

Herein, we introduced a biophysical tool to probe the dynamics of ACP with solvatochromic dyes. The attachment of pantetheine probes to two different ACPs enabled us to evaluate substrate sequestration and visualize chain-flipping upon interaction with a partner protein. NMR spectroscopy has previously been used to demonstrate that type I ACPs do not demonstrate sequestration; the present methods verified those findings.[6] However, the probes used in this study are not fatty acids, and type I ACPs might behave differently in the context of their synthase. Nevertheless, we have developed a simple and quick technique to visualize protein–protein interactions between ACP and partner enzymes. By matching EcACP with EcKASII, we demonstrated both selectivity and a sensitive readout for protein–protein interactions. The development of a solvatochromic cross-linking probe with novel dual-purpose functionalization allowed us to validate chain-flipping activity as a source of increased solvatochromic response. Finally, single-molecule fluorescence reports the outcome of individual chain-flipping events, with lifespan comparisons that indicate selectivity between EcACP and EcKASII as stabilized by protein–protein interactions.

Solvatochromic pantetheine probes also enable sequestration studies of other carrier proteins, including those from polyketide and nonribosomal-peptide biosynthetic pathways. Furthermore, these tools pave the way for dynamic studies of protein–protein interactions between the various partners of carrier proteins in type II synthases. Facile access to these probes allows for their broad use, such as the selection of new catalytic partners for synthetic biology. The combination of this technique with time-correlated single photon counting fluorescence spectroscopy[25] or vibrational spectroscopy[26] will enable accurate modeling of the chain-flipping phenomenon. Another potential application includes the use of these probes as a "turn-on" dye for ACP fusion proteins to quickly visualize their cellular localization.

Received: August 26, 2014
Published online: October 29, 2014

Keywords: acyl carrier protein · chain-flipping mechanism · fatty acid synthase · fatty acids · solvatochromism

[1] C. Nguyen, R. W. Haushalter, D. J. Lee, P. R. L. Markwick, J. Bruegger, G. Caldara-Festin, K. Finzel, D. R. Jackson, F. Ishikawa, B. O'Dowd, J. A. McCammon, S. J. Opella, S.-C. Tsai, M. D. Burkart, *Nature* **2014**, *505*, 427–431.
[2] D. M. Byers, H. Gong, *Biochem. Cell Biol.* **2007**, *85*, 649–662.
[3] J. Crosby, M. P. Crump, *Nat. Prod. Rep.* **2012**, *29*, 1111–1137.
[4] G. A. Zornetzer, B. G. Fox, J. L. Markley, *Biochemistry* **2006**, *45*, 5217–5227.
[5] D. I. Chan, D. P. Tieleman, H. J. Vogel, *Biochemistry* **2010**, *49*, 2860–2868.
[6] a) E. Płoskoń, C. J. Arthur, S. E. Evans, C. Williams, J. Crosby, T. J. Simpson, M. P. Crump, *J. Biol. Chem.* **2008**, *283*, 518–528; b) P. Wattana-amorn, C. Williams, E. Ploskoń, R. J. Cox, T. J. Simpson, J. Crosby, M. P. Crump, *Biochemistry* **2010**, *49*, 2186–2193.

[7] a) G. Loving, B. Imperiali, *J. Am. Chem. Soc.* **2008**, *130*, 13630 – 13638; b) G. S. Loving, M. Sainlos, B. Imperiali, *Trends Biotechnol.* **2010**, *28*, 73 – 83.
[8] a) C. Reichardt, *Chem. Rev.* **1994**, *94*, 2319 – 2358; b) J. J. La Clair, *Angew. Chem. Int. Ed.* **1998**, *37*, 325 – 329; *Angew. Chem.* **1998**, *110*, 339 – 343.
[9] A. S. Worthington, M. D. Burkart, *Org. Biomol. Chem.* **2006**, *4*, 44 – 46.
[10] M. S. Alexiou, V. Tychopoulos, S. Ghorbanian, J. H. P. Tyman, R. G. Brown, P. I. Brittain, *J. Chem. Soc. Perkin Trans. 2* **1990**, 837 – 842.
[11] S. Fery-Forgues, J.-P. Fayet, A. Lopez, *J. Photochem. Photobiol. A* **1993**, *70*, 229 – 243.
[12] D. A. Hinckley, P. G. Seybold, D. P. Borris, *Spectrochim. Acta Part A* **1986**, *42*, 747 – 754.
[13] J. Beld, E. C. Sonnenschein, C. R. Vickery, J. P. Noel, M. D. Burkart, *Nat. Prod. Rep.* **2014**, *31*, 61 – 108.
[14] D. Post-Beittenmiller, J. G. Jaworski, J. B. Ohlrogge, *J. Biol. Chem.* **1991**, *266*, 1858 – 1865.
[15] F. Ishikawa, R. W. Haushalter, D. J. Lee, K. Finzel, M. D. Burkart, *J. Am. Chem. Soc.* **2013**, *135*, 8846 – 8849.
[16] A. K. Joshi, L. Zhang, V. S. Rangan, S. Smith, *J. Biol. Chem.* **2003**, *278*, 33142 – 33149.
[17] J. E. Cronan, *Biochem. J.* **2014**, *460*, 157 – 163.
[18] A. Masoudi, C. R. H. Raetz, P. Zhou, C. W. Pemble IV, *Nature* **2014**, *505*, 422 – 426.
[19] A. Mainz, T. L. Religa, R. Sprangers, R. Linser, L. E. Kay, B. Reif, *Angew. Chem. Int. Ed.* **2013**, *52*, 8746 – 8751; *Angew. Chem.* **2013**, *125*, 8909 – 8914.
[20] G. D'Agnolo, I. S. Rosenfeld, P. R. Vagelos, *J. Biol. Chem.* **1975**, *250*, 5289 – 5294.
[21] a) A. S. Worthington, H. Rivera, J. W. Torpey, M. D. Alexander, M. D. Burkart, *ACS Chem. Biol.* **2006**, *1*, 687 – 691; b) J. Beld, J. L. Blatti, C. Behnke, M. Mendez, M. D. Burkart, *J. Appl. Phycol.* **2014**, *26*, 1619 – 1629.
[22] M. Leibundgut, S. Jenni, C. Frick, N. Ban, *Science* **2007**, *316*, 288 – 290.
[23] W. E. Moerner, S. W. Hell, E. Betzig, Nobel Prize in Chemistry 2014.
[24] D. Pappas, S. M. Burrows, R. D. Reif, *TrAC Trends Anal. Chem.* **2007**, *26*, 884 – 894.
[25] A. M. McLean, E. Socher, O. Varnavski, T. B. Clark, B. Imperiali, T. Goodson III, *J. Phys. Chem. B* **2013**, *117*, 15935 – 15942.
[26] M. N. R. Johnson, C. H. Londergan, L. K. Charkoudian, *J. Am. Chem. Soc.* **2014**, *136*, 11240 – 11243.

